Antitumor effect after radiofrequency ablation of murine hepatoma is augmented by an active variant of CC chemokine ligand 3/macrophage inflammatory protein-1a

doi: 10.1158/0008-5472.CAN-10-0096

Antitumor Effect after Radio-Frequency Ablation of Murine Hepatoma is Augmented by an Active Variant of CC Chemokine Ligand 3/Macrophage Inflammatory Protein-1alpha

Noriho Iida,[1] Yasunari Nakamoto,[1] Tomohisa Baba,[2] Hidetoshi Nakagawa,[1] Eishiro Mizukoshi,[1] Makoto Naito,[3] Naofumi Mukaida[2] and Shuichi Kaneko[1]

[1]Disease Control and Homeostasis, Graduate School of Medical Science, [2]Division of Molecular Bioregulation, Cancer Research Institute, Kanazawa University, Kanazawa, [3]Division of Cellular and Molecular Pathology, Niigata University Graduate School of Medicine, Niigata, Japan;

Running title: MIP-1α Augmented Antitumor Effect after Radio-Frequency Ablation

Key Words: Chemokines, Dendritic Cells, Radio-Frequency Ablation, Hepatoma, Tumor Immunity

Footnotes:

Address corresponding to: Shuichi Kaneko, M.D., PhD, Disease Control and Homeostasis, Graduate School of Medical Science, Kanazawa University, 13-1 Takara-machi, Kanazawa 920-8641, Japan. Phone, 81-76-265-2235; Fax, 81-76-234-4250; E-mail, skaneko@m-kanazawa.jp

ABSTRACT

Several chemokines are used for immunotherapy against cancers because they can attract immune cells such as dendritic and cytotoxic T cells to augment immune responses. Radio-frequency ablation (RFA) is used to locally eliminate cancers such as hepatocellular carcinoma (HCC), renal cell carcinoma, and lung cancer. Because HCC often recurs even after an eradicative treatment with RFA, additional immunotherapy is necessary. We treated tumor-bearing mice by administering ECI301, an active variant of CC chemokine ligand 3 (CCL3), after RFA. Mice were injected subcutaneously with BNL, a murine hepatoma cell line, in the bilateral flank. After the tumor became palpable, RFA was performed on the tumor of one flank with or without ECI301. RFA alone eliminated the treated ipsilateral tumors and retarded the growth of contralateral non-RFA-treated tumors accompanied with massive T-cell infiltration. Injection of ECI301 augmented RFA-induced antitumor effect against non-RFA-treated tumors when administered to wild-type or CCR5-deficient but not CCR1-deficient mice. ECI301 also increased CCR1-expressing $CD11c^+$ cells in peripheral blood and RFA-treated tumors after RFA. Deficiency of CCR1 impairs accumulation of $CD11c^+$, $CD4^+$, and $CD8^+$ cells in RFA-treated tumors. Furthermore, in IFN-γ-enzyme-linked immunospot assay, ECI301 augmented tumor-specific responses after RFA whereas deficiency of CCR1 abolished this augmentation. Thus, we proved that ECI301 further augments RFA-induced antitumor immune responses in a CCR1-dependent manner.

INTRODUCTION

Chemokines are a class of candidate molecules for immunotherapy. Chemokines are presumed to play an essential role in the regulation of leukocyte trafficking and dendritic cell: T cell interactions (1-4). In animal experiments, intratumoral use of chemokines, such as monocyte chemoattractant protein (MCP)-1/CCL2, macrophage inflammatory protein (MIP)-1α/CCL3, or MIP-3α/CCL20, succeed in decreasing tumorigenesis accompanied with increase in the numbers of tumor-infiltrating dendritic, natural killer, or T cells (5-7). Thus, application of chemokines in immunotherapy is promising but needs further refinement before they can be used in clinical situations.

Radio-frequency ablation (RFA) is an eradicative treatment against cancers, such as hepatocellular carcinoma (HCC), renal cell carcinoma, and lung cancer. RFA of HCC can generate HCC-specific T cells in peripheral blood (8). Activation of dendritic cells in human peripheral blood is also observed after this treatment (9). Thus, RFA can induce immunogenic tumor cell death and subsequently tumor-specific immune responses (8-11). However, multicentric development of HCC in the cirrhotic liver frequently results in tumor recurrence even after the apparent curative treatment of HCC by RFA (12). These observations suggest that RFA-induced tumor-specific immune responses are often not sufficient to prevent tumor recurrence. Thus, additional treatment modalities are required to augment HCC-specific immune responses.

CCL3/MIP-1α can augment immune responses but problems arise because of its tendency to form large aggregates at high concentrations when administered systemically. Unlike human naïve CCL3, BB-10010 is generated by a single amino acid substitution of Asp26 to Ala and exhibits similar biological potencies, but rarely forms large aggregates (13). Based on its activity to mobilize bone marrow cells to peripheral blood, randomized clinical trials were performed to examine whether the combined administration of BB-10010 and chemotherapeutic agents can protect against chemotherapy-induced neutropenia. However, the myeloprotective effects of BB-10010 were not sufficient to warrant its use with chemotherapy (14). Concomitantly, several lines of evidence reveal that the administration of human recombinant CCL3 can mobilize activated T-cell and dendritic cell precursors into circulation (15, 16).

ECI301, which has the same amino acid sequence as BB-10010, was generated using the fission yeast (*Schizosaccharomyces pombe*) expression system. ECI301 can augment irradiation-induced tumor regression when administered systemically to mice bearing multiple subcutaneous tumors (17). Of interest is the fact that the effects were observed in both unirradiated as well as irradiated tumors. Thus, systemic ECI301 treatment can augment irradiation-induced tumor-specific systemic immunity. These observations prompted us to investigate the effects of ECI301 on RFA-treated mice. Here, we demonstrate that ECI301 further augments RFA-induced antitumor immune responses in a CCR1-dependent manner.

MATERIALS AND METHODS

Mice

Specific pathogen-free 7- to 9-week-old female BALB/c mice were purchased from Charles River Japan (Yokohama, Japan) and designated as wild-type (WT) mice. BALB/c-*nu/nu* mice were purchased from CLEA Japan. CCR1-deficient ($CCR1^{-/-}$) mice were a gift from Dr. Philip M. Murphy [National Institute of Allergy and Infectious Disease, National Institute of Health (NIAID, NIH), Bethesda, MD, USA], CCR5-deficient ($CCR5^{-/-}$) mice were a gift from Dr. Kouji Matsushima (Department of Molecular Preventive Medicine, Tokyo University, Tokyo, Japan). All mice were backcrossed to BALB/c mice for 8 to 10 generations. All animal experiments were performed under specific pathogen-free conditions in accordance with the Guidelines for the Care and Use of Laboratory Animals of Kanazawa University (Japan).

Tumor cell line

A murine HCC cell line, BNL 1ME A.7R.1 (BNL) was purchased from American Type Culture Collection in 1998 and kept at low passage throughout the study. The cells were screened for bacteria, fungus and mycoplasma contamination by direct culture method in 2006 before a start of the study. The cells were cultured in Dulbecco's modified essential medium (Sigma Chemical Co., St. Louis, MO) containing 10% fetal bovine serum, 0.1 mM nonessential amino acids, 1 μM sodium pyruvate, 2 mM L-glutamine, 50 μg/ml streptomycin and 100 U/ml penicillin (Gibco, Long Island, NY).

Animal models

ECI301 was generated as previously described and provided by Effector Cell Institute, Inc (Tokyo, Japan). (17, 18). Left and right flanks of 7- to 9-week-old female WT, $CCR1^{-/-}$, $CCR5^{-/-}$ and *nu/nu* mice were injected subcutaneously with 5×10^5 BNL cells in 100 μl PBS. Fourteen days later, when tumor size reached a diameter of 6–8 mm, tumors of one flank were treated using a radio frequency (RF) generator (RITA 500PA; RITA Medical Systems, Fremont, CA) and needle as described below. On day 0, 2, 4 after RFA, 20 μg of ECI301 in 100 μl PBS was injected intravenously via the tail vein, while mice treated with RFA alone were injected

with 100μl of PBS. Untreated tumor-bearing mice were used as controls. In another schedule, 2 μg of ECI301 in 100 μl PBS was injected intravenously from day 0 to 4 (5 consecutive days). Sizes of non-RFA-treated tumors on the contralateral flank were evaluated twice a week using calipers and tumor volumes were calculated using the following formula:

Tumor volume (mm^3) = (longest diameter) × (shortest diameter)^2/2

RFA-treated or non-RFA-treated tumors were excised at the indicated time intervals for immunohistochemical analysis and quantitative real-time RT-PCR. Spleens and peripheral blood were removed from the mice at the indicated time intervals for flow cytometric analysis and enzyme-linked immunospot assay (ELISPOT).

RFA

Mice were anesthetized by intraperitoneal injection of Somnopentyl® (Schering-Plough Animal Health, Boxmeer, Netherlands) and carefully shaved in the tumor area. After placing the mice onto an aluminum plate attached with an electricity-conducting pad, an RFA needle of expandable electrode with maximum dimension of 20 mm (70SB 2 cm; RITA Medical Systems) was inserted into the middle of the tumors, and expanded at 2 or 3 mm. RFA treatments were performed using an RF generator at a power output of 25 W for 1.5 min and the temperature of the needle tips reached 70−80°C.

Immunohistochemical analysis

The removed tumor tissues were embedded in Sakura Tissue-Tek OCT compound (Sakura Finetek, Torrance, CA) as frozen tissues. Cryostat sections of the frozen tissues were fixed with 4% paraformaldehyde (PFA) in PBS and stained with rat anti-mouse CD4 (BD Biosciences, San Diego, CA, USA), rat anti-mouse CD8a (BD Biosciences), hamster anti-mouse CD11c (BD Biosciences), and rat anti-mouse F4/80 antibodies (Serotec, Oxford, UK) overnight at 4°C. The sections were then incubated with biotinylated rabbit anti-rat IgG (Dako Cytomation, Tokyo, Japan) or biotinylated mouse anti-hamster IgG (BD Biosciences) for 1 h at room temperature. The immune complexes were visualized using the Catalyzed Signal Amplification System (Dako Cytomation) or the Vectastain Elite ABC and DAB substrate kits (Vector Laboratories, Burlingame, CA, USA) according to the manufacturer’s instructions. As a negative control, rat

IgG (Cosmo Bio, Tokyo, Japan), or hamster IgG (BD Biosciences) was used instead of specific primary antibodies. The numbers of positive cells in each animal were counted in 10 randomly selected fields at 400-fold magnification by an examiner without any prior knowledge of the experimental procedures.

Double-color immunofluorescence analysis

Tumor tissues were embedded in the OCT compound as frozen tissues. After fixation with 4% PFA/PBS, cryostat sections were stained with the combinations of anti-CD4 and goat anti-mouse CCR1 (Santa Cruz Biotechnology, Santa Cruz, CA), anti-CD8a and anti-CCR1, anti-F4/80 and anti-CCR1, PE-conjugated hamster anti-CD11c (BD Biosciences) and anti-CCR1, anti-F4/80 and goat anti-mouse CCL3 (R&D Systems, Minneapolis, MN), and anti-F4/80 and goat anti-mouse CCL4 antibodies (R&D). After extensive washing, AF488 donkey anti-rat IgG (Invitrogen, Carlsbad, CA) was used as a secondary antibody to detect $CD4^+$, $CD8a^+$, or $F4/80^+$ cells. Simultaneously, AF546- or AF488-donkey anti-goat IgG (Invitrogen) was used to detect $CCR1^+$, $CCL3^+$, or $CCL4^+$ cells. The sections were observed using a confocal microscope (LSM 510 META, Zeiss, NY).

Quantitative real-time RT-PCR

Total RNA was extracted from the resected tumor using RNeasy Mini kit (Qiagen, Hilden, Germany) according to the manufacturer's instructions. After treating the RNA preparations with ribonuclease-free deoxyribonuclease (DNase) I (Qiagen) to remove residual DNA, cDNA was synthesized as described previously (19). Quantitative real-time PCR was performed on a StepOne™ Real-Time PCR System (Applied Biosystems, Foster City, CA) using the comparative C_T quantification method. TaqMan® Gene Expression Assays (Applied Biosystems) containing specific primers and probes (accession numbers: CCL3, Mm00441258_ml; CCL4, Mm00443111_m1; CCL5, Mm01302428_ml; GAPDH, Mm99999915_g1) and TaqMan® Fast Universal PCR Master Mix were used with 10 ng cDNA to quantify the expression levels of CCL3, CCL4, and CCL5. Reactions were performed for 20 s at 95°C followed by 40 cycles of 1 s at 95°C and 20 s at 60°C. GAPDH was amplified as an internal control and their C_T values were subtracted from C_T values of the target genes (ΔC_T).

ΔC_T values of tumors after RFA with or without ECI301 were compared to ΔC_T values of tumors of untreated mice.

Enzyme-linked immunospot assay (ELISPOT)

To prepare tumor lysates, BNL or CT26 cells were suspended in PBS and subjected to four cycles of rapid freezing in liquid nitrogen and thawing at 55°C. The lysate was spun at 15,000 rpm to remove particulate cellular debris. After harvesting murine spleens on day 21 after RFA, mononuclear cells were isolated by centrifugation through a Histopaque-1083 density gradient (Sigma Chemical Co.). ELISPOT was performed using an IFN-γ-ELISPOT kit (Mabtech, Nacka, Sweden). Ninety-six-well plates coated with anti-mouse interferon-γ antibody were blocked for 2 h with RPMI 1640 medium (Sigma Chemical Co.) containing 10% FBS. Two hundred and fifty thousand splenic mononuclear cells were added in triplicate cultures of RPMI 1640 containing 10% FBS together with BNL or CT26 lysates at a tumor cell-to-mononuclear cell ratio of 2:1. After 48 h of culture, the plates were washed eight times with sterile PBS and further incubated 2 h with biotinylated anti-mouse IFN-γ antibody. After another eight washes, alkaline phosphatase-conjugated streptavidin was added to these plates and incubated for 1 hr. Finally the spots were developed with NBT/BCIP solution. The numbers of specific spots were determined by subtracting the number of spots in wells without lysates from the number of spots in wells with tumor lysates. Wells were considered as positive if they had more than 10 spots per well and were at least twofold greater than control.

Flow cytometric analysis

After harvesting blood samples from mice, mononuclear cells were isolated by centrifugation through a Histopaque-1083 density gradient (Sigma Chemical Co.). The resultant single-cell preparations were stained with various combinations of APC-labeled anti-CD8, APC-labeled anti-CD11c, FITC-labeled anti-CD4 (BD Biosciences), PE-labeled anti-CCR1 (Santa Cruz Biotechnology), and FITC-labeled anti-F4/80 monoclonal antibodies (Serotec). APC-rat IgG, APC-hamster IgG, and FITC-rat IgG were used as isotype controls (BD Biosciences). For each determination, at least 20,000 stained cells were analyzed on a FACSCalibur system (BD Biosciences). The data were expressed as a proportion of positive cells (compared to cells

stained with an irrelevant control antibody).

Depletion of macrophages/monocytes

Clodronate liposome was prepared and systemic depletion of monocytes/macrophages was performed as previously described (20, 21). WT mice were intraperitoneally injected with 200μl of clodronate liposome 5 times; days -2, 0, 3, 6, and 10 after RFA treatment. Depletion of CD11c-negative monocytes in blood was confirmed by flow cytometry after injection of clodronate liposome.

Statistical analysis

Mean and SD or SE were calculated for the obtained data. Data were analyzed statistically using one-way ANOVA followed by the Fisher's PLSD test, except for the data of tumor growth which were analyzed with two-way ANOVA. A p value less than 0.05 was considered statistically significant.

RESULTS

ECI301 augments RFA-induced antitumor effects.

In order to investigate the effects of RFA against RFA-treated and non-RFA-treated tumors, each bilateral flank of BALB/c mice was injected with 5×10^5 of BNL cells. Fourteen days later, when tumor size reached a diameter of 6–8 mm, tumors of one flank were treated by RFA treatment. On the day after RFA, ulceration occurred in RFA-treated tumors, and these tumors started to shrink (data not shown). On day 14 after RFA, RFA-treated tumors were covered with scars without any macroscopic tumors (Fig. 1A). Moreover, RFA treatment also retarded the growth of contralateral non-RFA-treated tumors compared with the tumors in untreated mice (Fig. 1B and C). Twenty μg/mouse of ECI301 administered on day 0, 2, 4 after RFA augmented RFA-induced growth retardation of contralateral non-RFA-treated tumors (Fig. 1B and C). Furthermore, non-RFA-treated tumors completely disappeared in 2 of 15 mice treated with RFA and ECI301 but not in the other treatment groups (Fig. 1B and C). Therapeutic effects were observed, even when 2 μg/mouse of ECI301 was injected consecutively for 5 days from day 0 to 4 after RFA. On the contrary, administration of ECI301 without RFA did not result in a significant decrease in tumor size (Fig. 1C). These observations suggest that ECI301 can augment RFA-induced antitumor effects but fails to induce antitumor effects by itself.

Deficiency of CCR1 abrogates increased antitumor effect of ECI301 after RFA.

ECI301 utilizes two distinct chemokine receptors, CCR1 and CCR5. In order to elucidate the roles of these chemokine receptors, either tumor-bearing $CCR1^{-/-}$ or $CCR5^{-/-}$ mice was similarly treated with RFA plus ECI301. RFA retarded the growth of non-RFA-treated tumors in $CCR1^{-/-}$ mice similar to that in WT mice, but ECI301 failed to further accentuate RFA-induced growth retardation of non-RFA-treated tumors (Fig. 2A). In contrast, ECI301 augmented RFA-mediated inhibition of non-RFA-treated tumors in $CCR5^{-/-}$ mice, resulting in complete tumor eradication in 1 of 6 mice (Fig. 2B). These observations indicate that CCR1- but not CCR5-expressing cells play an important role in ECI301-induced augmentation of tumor regression after RFA.

ECI301 increases CCR1-expressing cells in peripheral blood and RFA-treated tumors

after RFA.

The reported capacity of CCL3 to mobilize leukocytes into peripheral blood (15, 16), prompted the investigation of the effects of ECI301 on peripheral blood. RFA alone had few effects on the numbers of CCR1-expressing cells, but subsequent ECI301 administration increased the numbers of CCR1-expressing cells in peripheral blood, particularly $CD11c^+$ but not $CD4^+$ or $CD8^+$ cells (Fig. 3). Because immune cells need to accumulate into RFA-treated tumors at an early stage in order to initiate adaptive immune responses, CCR1 expression by tumor-infiltrating cells into RFA-treated tumors was examined 8 h after treatment. RFA-induced $CD4^+$, $CD8^+$, $CD11c^+$, and $F4/80^+$ cell infiltrations into RFA-treated tumors was greater than those into tumors of untreated mice. Moreover, ECI301 further increased the numbers of tumor-infiltrating $CD4^+$, $CD8^+$ and $CD11c^+$ cells into RFA-treated tumors compared with the numbers of these cells infiltrating tumors treated with RFA alone (Fig. 4A and B). In RFA-treated tumors, most $CD11c^+$ and $F4/80^+$ cells expressed CCR1, whereas a few $CD4^+$ and $CD8^+$ cells expressed CCR1 (Fig. 4C). Furthermore, ECI301-induced $CD4^+$, $CD8^+$, and $CD11c^+$ cell infiltrations into ablated tumors was lesser in $CCR1^{-/-}$ mice than in WT mice, whereas $F4/80^+$ cells infiltrated RFA-treated tumors in $CCR1^{-/-}$ mice and WT mice to a similar extent (Fig. 4D). These observations suggest that ECI301 augments RFA-induced $CD4^+$, $CD8^+$ and $CD11c^+$ cell infiltrations into RFA-treated tumors in a CCR1-dependent manner.

ECI301 increases intratumoral expression of CCL3 after RFA.

We demonstrated that $CCR1^+$ cells were mobilized into blood by intravenously administered ECI301. However, concentration of ECI301 in blood can go down rapidly as time passes (the peak is 5 minutes, and the half-life is less than 2 hours; unpublished data from Effector Cell Institute), allowing ECI301-mobilized $CCR1^+$ cells possibly to migrate into tissues where chemokines are highly produced. In order to prove this point, chemokine expression in RFA-treated tumors was examined. RFA plus ECI301 treatment increased CCL3 mRNA expression level 6 hours after RFA. Moreover, 24 hours after the treatment, CCL3 and CCL4 mRNA expression level became almost 10-fold higher in tumors treated with RFA alone than in tumors of untreated mice, and ECI301 further increased the mRNA expression level of these chemokines in RFA-treated tumors (Fig. 5A). CCL3 and CCL4 were detected in

tumor-infiltrating F4/80$^+$ cells (Fig. 5B). These observations indicated that RFA treatment caused local production of CCL3 and CCL4 in RFA-treated tumors and ECI301 further increases the expression of these chemokines. As the concentration of ECI301 in blood decreases, chemokines produced locally in RFA-treated tumor can attract CCR1-expressing CD11c$^+$ cells, thereby indirectly inducing CCR1-negative CD4$^+$ and CD8$^+$ cell infiltrations.

ECI301 augments RFA-induced tumor-specific immune responses accompanied with T-cell infiltrations into non-RFA-treated tumors.

Non-RFA-treated tumors were analyzed histologically to clarify the mechanisms underlying the CCR1-dependent inhibitory effect of RFA plus ECI301 treatment against these tumors. Although a few CD4$^+$ or CD8$^+$ cells were observed in the tumors of untreated mice, RFA treatment increased the numbers of CD4$^+$ and CD8$^+$ cells in the non-RFA-treated tumors 3 days after RFA. ECI301 further augmented RFA-induced CD4$^+$ and CD8$^+$ cell infiltration into non-RFA-treated tumors (Fig. 6A and B). However, only a marginal number of CD11c$^+$ or F4/80$^+$ cells infiltrated into non-RFA-treated tumors of mice treated with RFA alone or RFA plus ECI301-treated mice (data not shown). Based on these findings, we hypothesized that ECI301-augmented tumor regression after RFA may be associated with T-cell-mediated antitumor immune responses. To clarify this point, BALB/c-background nu/nu mice were treated by RFA with or without ECI301. Deficiency of T cells abrogated tumor-inhibitory effect of ECI301 as well as RFA-induced antitumor effect (Fig. 6C). Thus, both ECI301- and RFA-induced tumor regression require T cell-mediated antitumor immune response.

However, CD4$^+$ or CD8$^+$ T cells rarely expressed CCR1 in blood and RFA-treated tumors. CCR1$^+$ cells in the RFA-treated tumors were CD11c$^+$ cells and F4/80$^+$ cells, and only the former accumulates into the RFA-treated tumor in a CCR1-dependent manner. These findings suggest that CCR1-positive CD11c$^+$ cells may activate antitumor T-cell responses and indirectly induce tumor retardation. Accordingly, we next examined the effect of depletion of monocytes/macrophages on ECI301-augmented tumor regression. Intraperitoneal injection of clodronate liposome depleted CD11c-negative monocytes in blood, although it didn't change the number of CD11c$^+$ cells (data not shown). Depletion of these CD11c-negative monocytes didn't cause any effects on ECI301-enhanced tumor regression, indicating that

ECI301-augmented antitumor T-cell immunity was independent of CD11c-negative monocytes (Fig. 6C).

Finally, in order to prove the presence of systemic adaptive immune responses, IFN-γ ELISPOT assay was performed using mononuclear cells from the spleen. A greater number of spots against BNL cell lysates but not against CT26 cell lysates were generated by RFA plus ECI301-treated mice than that by mice treated with RFA alone or untreated mice. Moreover, ablation of *CCR1* but not *CCR5* gene reduced the number of spots against BNL cell lysates even when the mice were treated with RFA plus ECI301 (Fig. 6D). These observations suggest that ECI301 can further augment RFA-induced tumor-specific adaptive immune responses and subsequent tumor retardation in a CCR1-dependent manner.

DISCUSSION

HCC occurs predominantly in individuals with chronic liver disease related to either hepatitis B or C virus infections (22-24). In addition to surgical resection, RFA treatment has been developed to eradicate solitary HCC lesions (25). RFA of HCC induces specific T-cell responses against liver tumors in human and rabbit (8, 11). Moreover, activated dendritic cells were detected in peripheral blood of HCC patients after RFA (9). These previous reports indicate that RFA treatment can induce antitumor immune responses against HCC (8-11). Likewise, we observed that RFA treatment generated tumor-specific IFN-γ-producing cells and inhibited the growth of non-RFA-treated tumors accompanied with massive T-cell infiltration into these tumors. However, even after successful ablation of HCC lesion by RFA, tumor recurrence often occurs probably because HCC develops in a multicentric manner in the cirrhotic liver (12). These observations indicate that RFA-induced augmentation in immune response may not be sufficient to prevent tumor recurrence. Thus, a novel therapeutic modality is required to further augment RFA-induced tumor-specific immune responses. Here, we demonstrated that combined administration of ECI301 and RFA can augment tumor-specific immune responses against HCC.

Several chemokines are used for immunotherapy against cancers because they can attract immune cells such as dendritic and cytotoxic T cells to augment tumor specific immune responses (26). However, some chemokines can simultaneously attract myeloid-derived suppressor and regulatory T cells to promote neovascularization and induce immunosuppressive microenvironments (26-28). The double-edged activities of chemokines frequently preclude their use for tumor immunotherapy. Moreover, most chemokines exhibit a bell-shaped dose-response curve with a narrow effective dose window. Thus, determination of an optimal dose of chemokines is important to elicit efficient antitumor responses (29). Several lines of evidence demonstrate that intratumoral use of CCL3 reduces tumorigenicity (6, 30). Furthermore, there are no reports demonstrating that use of CCL3 can promote tumor progression. We observed that systemic administration of ECI301 without RFA treatment induced neither reduction nor progression of tumors. On the contrary, systemic injection of ECI301 after RFA can inhibit growth of non-RFA-treated tumors in the contra-lateral side.

ECI301-enhanced tumor regression after RFA was both CCR1-dependent and T cell-dependent, but T cells rarely expressed CCR1 in blood and RFA-treated tumors. Because depletion of monocytes/macrophages didn't affect the retardation of ECI301-treated tumors, CCR1-expressing $CD11c^+$ DC might activate antitumor T-cell responses and indirectly induce tumor retardation via some mechanisms such as antigen-presentation and cytokine-production. ECI301 mobilized a large number of $CCR1^+$ cells into blood, and these mobilized cells may be attracted into highly CCL3-producing RFA-treated tumors and cause increased number of tumor-infiltrating $CCR1^+CD11c^+$ DC. Thus, $CCR1^+$ precursors in blood and $CCR1^+CD11c^+$ tumor-infiltrating DC might play important roles in ECI301-augmented antitumor effects (31-33).

ECI301 could not increase the number of $F4/80^+$ cells in the RFA-treated tumor sites. Accumulation of $F4/80^+$ cells in the tumor treated with ECI301 plus RFA was also independent of CCR1. $F4/80^+$ cells, which might include a large number of macrophages/monocytes, are usually attracted into the tumor by CCL2, CCL4, and CCL5 that are produced in the tumor sites. CCR2, the receptor for CCL2, and CCR5, the receptor for CCL4 and CCL5, might be responsible for migration of monocytes/macrophages (27, 34-36). However, it is still unclear whether monocytes/macrophages utilize CCR2 or CCR5 after massive tumor cell death caused by the treatments such as RFA, because tumor cell death induces different profile of chemokine production in the tumors (4). Although ECI301 didn't directly induce migration of $F4/80^+$ cells, the mechanism underlying the infiltration of $F4/80^+$ macrophages remains to be elucidated.

Breaking tolerance for tumor cells is necessary for induction of antitumor immunity. Several independent groups have suggested multiple mechanisms underlying immunogenic tumor cell death induced by anti-cancer chemotherapy or radiation therapy (37-40). Anthracyclin causes apoptosis along with translocation of calreticulin to the apoptotic tumor cell surface. Calreticulin exposure augments phagocytosis of apoptotic cancer cells by dendritic cells with an eventual increase in immune response (37, 38). Chemotherapy or irradiation kills tumor cells to release high mobility group box 1 (HMGB1). Released HMGB1 activates dendritic cells after binding to toll-like receptor 4 expressed by these cells (39). Apoptosis induced by local radiation therapy augments MHC class I expression by tumor cells, thereby facilitating their recognition by cytotoxic T cells (40). RFA induces the expression of heat shock

protein 70 and 90 on ablated tumor cells, and these proteins can activate TLR-expressing antigen presenting cells (41, 42). In addition, we demonstrated that RFA treatment alone caused local production of CCL3 in RFA-treated tumors accompanied with accumulation of T-cells and $CD11c^+$ DC. These mechanisms may also account for the observed RFA-induced generation of tumor-specific immune responses.

We revealed that combined treatment of ECI301 and RFA augmented antitumor-specific immune responses, thereby inhibiting the growth of non-RFA-treated tumors in a CCR1-dependent manner. Thus, combined treatment of ECI301 and RFA can prevent human HCC from recurring after RFA treatment. Absence of any severe adverse effects in mice (data not shown) may further warrant the clinical trial of ECI301 combined with RFA as a treatment regimen for HCC.

ACKNOWLEDGMENTS

We thank Dr. Philip M. Murphy (NIAID, NIH) and Dr. Kouji Matsushima (Tokyo University) for providing us with $CCR1^{-/-}$ and $CCR5^{-/-}$ mice, respectively.

REFERENCES

1. Luster AD. Chemokines-chemotactic cytokines that mediate inflammation. N Engl J Med 1998;338:436-45.
2. Castellino F, Huang AY, Altan-Bonnet G, Stoll S, Scheinecker C, Germain RN. Chemokines enhance immunity by guiding naïve $CD8^+$ T cells to sites of $CD4^+$ T cell-dendritic cell interaction. Nature 2006;440:890-5.
3. Sozzani S. Dendritic cell trafficking: more than just chemokines. Cytokine Growth Factor Rev 2005;16:581-92.
4. Iida N, Nakamoto Y, Baba T, et al. Tumor cell apoptosis induces tumor-specific immunity in a CC chemokine receptor 1-and 5-dependent manner in mice. J Leukoc Biol 2008;84:1001-10.
5. Tsuchiyama T, Nakamoto Y, Sakai Y, et al. Prolonged, NK cell-mediated antitumor effects of suicide gene therapy combined with monocyte chemoattractant protein-1 against hepatocellular carcinoma. J Immunol 2007;178:574-83.
6. Crittenden M, Gough M, Harrington K, Olivier K, Thompson J, Vile RG. Expression of inflammatory chemokines combined with local tumor destruction enhances tumor regression and long-term immunity. Cancer Res 2003;63:5505-12.
7. Furumoto K, Soares L, Engleman EG, Merad M. Induction of potent antitumor immunity by in situ targeting of intratumoral DCs. J Clin Invest 2004;113:774-83.
8. Zerbini A, Pilli M, Penna A, et al. Radiofrequency thermal ablation of hepatocellular carcinoma liver nodules can activate and enhance tumor-specific T-cell responses. Cancer Res 2006;66:1139-46.
9. Ali MY, Grimm CF, Ritter M, et al. Activation of dendritic cells by local ablation of hepatocellular carcinoma. J Hepatol 2005;43:817-22.
10. Brok MH, Sutmuller RP, Voort R, et al. In situ tumor ablation creates antigen source for the generation of antitumor immunity. Cancer Res 2004;64:4024-29.
11. Wissniowski TT, Hünsler J, Neureiter D, et al. Activation of tumor-specific T lymphocytes by radio-frequency ablation of the VX2 hepatoma in rabbits. Cancer Res 2003;63:6496-500.

12. Poon RT, Fan ST, Ng IO, Lo CM, Liu CL, Wong J. Different risk factors and prognosis for early and late intrahepatic recurrence after resection of hepatocellular carcinoma. Cancer 2000;89:500-7.
13. Hunter MG, Bawden L, Brotherton D, et al. BB-10010: an active variant of human macrophage inflammatory protein-1α with improved pharmaceutical properties. Blood 1995;86:4400-8.
14. Clemons MJ, Marshall E, Dürig J, et al. A randomized phase-II study of BB-10010 (macrophage inflammatory protein-1α) in patients with advanced breast cancer receiving 5-fluorouracil, adriamycin, and cyclophosphamide chemotherapy. Blood 1998;92:1532-40.
15. Zhang Y, Yoneyama H, Wang Y, et al. Mobilization of dendritic cell precursors into the circulation by administration of MIP-1α in mice. J Natl Cancer Inst 2004;96:201-9.
16. Taub DD, Conlon K, Lloyd AR, Oppenheim JJ, Kelvin DJ. Preferential migration of activated $CD4^+$ and $CD8^+$ T cells in response to MIP-1α and MIP-1β. Science 1993;260:355-8.
17. Shiraishi K, Ishiwata Y, Nakagawa K, et al. Enhancement of antitumor radiation efficacy and consistent induction of the abscopal effect in mice by ECI301, an active variant of macrophage inflammatory protein-1α. Clin Cancer Res 2008;14:1159-66.
18. Isoai A, Kimura H, Reichert A, et al. Production of D-amino acid oxidase of Trigonopsis variabilis in Schizosaccharomyces pombe and the characterization of biocatalysts prepared with recombinant cells. Biotechnol Bioeng 2002;80:22-32.
19. Lu P, Nakamoto Y, Nemoto-Sakai Y, et al. Potential interaction between CCR1 and its ligand, CCL3, induced by endogeneously produced interleukin-1 in human hepatomas. Am J Pathol 2003;162,:1249-58.
20. Lu P, Li L, Liu G, Rooijen N, Mukaida N, Zhang X. Opposite roles of CCR2 and CX3CR1 macrophages in alkali-induced corneal neovascularization. Cornea 2009;28:562-9.
21. Sadahira Y, Yasuda T, Yoshino T, et al. Impaired splenic erythropoiesis in phlebotomized mice injected with CL2MDP-liposome: an experimental model for studying the role of stromal macrophages in erythropoiesis. J Leukoc Biol 2000;68:464-70.
22. Tsukuma H, Hiyama T, Tanaka S, et al. Risk factors for hepatocellular carcinoma among patients with chronic liver disease. N Engl J Med 1993;328:1797-801.

23. Velázquez RF, Rodríguez M, Navascués CA, et al. Prospective analysis of risk factors for hepatocellular carcinoma in patients with liver cirrhosis. Hapatology 2003;37:520-7.
24. Okita K. Management of hepatocellular carcinoma in Japan. J Gastroenterol 2006;41:100-6.
25. Tateishi R, Shiina S, Ohki T, et al. Treatment strategy for hepatocellular carcinoma : expanding the indication for radiofrequency ablation. J Gastroenterol 2009;44 Suppl:142-6.
26. Homey B, Müller A, Zlotnik A. Chemokines: agents for the immunotherapy of cancer? Nat Rev Immnol 2002;2:175-84.
27. Balkwill F. Cancer and the chemokine network. Nat Rev Cancer 2004;4:540-50.
28. Dell'Agnola C, Biragyn A. Clinical utilization of chemokines to combat cancer: the double-edged sword. Expert Rev Vaccines 2007;6:267-83.
29. Tsuchiyama T, Nakamoto Y, Sakai Y, Mukaida N, Kaneko S. Optimal amount of monocyte chemoattractant protein-1 enhances antitumor effects of suicide gene therapy against hepatocellular carcinoma by M1 macrophage activation. Cancer Sci 2008;99:2075-82.
30. Nakashima E, Ova A, Kubota YA. A candidate for cancer gene therapy: MIP-1α gene transfer to an adenocarcinoma cell line reduced tumorigenesity and induced protective immunity in immunocompetent mice. Pharm Res 1996;13:1896-901.
31. Geissmann F, Manz MG, Jung S, Sieweke MH, Merad M, Ley K. Development of monocytes, macrophages, and dendritic cells. Science 2010;327:656-661.
32. Randolph GJ, Ochando J, Partida-Sánchez S. Migration of dendritic cell subsets and their precursors. Annu Rev Immunol 2008;26:293-316.
33. López-Bravo M, Ardavín C. In vivo induction of immune responses to pathogens by conventional dendritic cells. Immunity 2008;29:343-51.
34. Murdoch C, Muthana M, Coffelt SB, Lewis CE. The role of myeloid cells in the promotion of tumor angiogenesis. Nat Rev Cancer 2008;8:618-31.
35. Azenshtein E, Luboshits G, Shina S, et al. The CC chemokine RANTES in breast carcinoma progression: regulation of expression and potential mechanism of promalignant activity. Cancer Res 2002;62:1093-102.
36. Nesbit M, Schaider H, Miller TH, Herlyn M. Low-level monocyte chemoattractant protein-1 stimulation of monocytes leads to tumor formation in nontumorigenic melanoma cells. J Immunol 2001;166:6483-90.

37. Obeid M, Tesniere A, Ghiringhelli F, et al. Calreticulin exposure dictates the immunogenicity of cancer cell death. Nat Med 2007;13:54-61.
38. Casares N, Pequignot MO, Tesniere A., et al. Caspase-dependent immunogenicity of doxorubicin-induced tumor cell death. J Exp Med 2005;202:1691-701.
39. Apetoh L, Ghiringhelli F, Tesniere A, et al. Toll-like receptor 4-dependent contribution of the immune system to anticancer chemotherapy and radiotherapy. Nat Med 2007;13:1050-59.
40. Reits EA, Hodge JW, Herberts CA, et al. Radiation modulates the peptide repertoire, enhances MHC class I expression, and induces successful antitumor immunotherapy. J Exp Med 2006;203:1259-71.
41. Schueller G, Kettenbach J, Sedivy R, et al. Heat shock protein expression induced by percutaneous radiofrequency ablation of hepatocellular carcinoma in vivo. Int J Oncol 2004;24:609-13.
42. Nikfarjam M, Muralidharan V, Su K, Malcontenti-Wilson C, Christophi C. Patterns of heat shock protein (HSP70) expression and Kupffer cell activity following thermal ablation of liver and colorectal liver metastasis. Int J Hyperthermia 2005;21:319-32.

FIGURE LEGENDS

Figure 1. ECI301-induced augmentation of antitumor effects after RFA.

WT mice were injected subcutaneously with 5×10^5 BNL cells into the left and right flanks. Fourteen days later, when tumors became palpable, tumors of one flank were treated using the RFA generator and needle. On day 0, 2, 4 after RFA, 20 μg of ECI301 in 100 μl PBS was injected intravenously into each mouse, while mice treated with RFA alone were injected with 100 μl PBS. Tumor-bearing untreated mice were observed as controls. (A) Macroscopic appearances of the mice on day 14 after RFA are shown. Arrow heads indicate the scar after RFA. Representative results are from at least 10 mice in each group. (B) Non-RFA-treated tumor volumes (mean and SE) after RFA with or without ECI301 were measured twice a week. $*p < 0.05$; $***p < 0.001$. (C) Volumes of non-RFA-treated tumors on day 14 after RFA. In addition to the groups described in Fig. 1B, tumor volumes (mean and SE) were determined in animals receiving 2 μg of ECI301 in 100 μl PBS intravenously from day 0 to 4 (5 consecutive days) after RFA and those receiving 20 μg of ECI301 alone without RFA. $*p < 0.05$; $**p < 0.01$; $***p < 0.001$ compared with untreated mice.

Figure 2. Deficiency of CCR1 abrogated ECI301 augmented antitumor effects after RFA.

$CCR1^{-/-}$ or $CCR5^{-/-}$ mice were inoculated with BNL cells and treated as described in the legend to figure 1. Non-RFA-treated tumor volumes (mean and SE) were measured twice a week on $CCR1^{-/-}$ (A) or $CCR5^{-/-}$ mice (B). $*p < 0.05$; $**p < 0.01$.

Figure 3. ECI301 increased CCR1-expressing cells in peripheral blood.

Peripheral blood sample was harvested 8 h after RFA. Mononuclear cells were separated and stained with indicated antibodies as described in Materials and Methods. The percentages of $CCR1^+$, $CCR1^+CD4^+$, $CCR1^+CD8^+$, $CCR1^+CD11c^+$, or $CCR1^+F4/80^+$ cells were determined and are indicated. Mean and SD were calculated and are shown here (n = 3). $*p < 0.05$.

Figure 4. ECI301 increased infiltration of CCR1-expressing leukocytes into RFA-treated

tumors after RFA.

RFA-treated tumors were removed from WT or CCR1$^{-/-}$ mice 8 h after RFA. (A), (B), and (D) Immunohistochemical analysis was performed using anti-CD4, anti-CD8a, anti-CD11c, or anti-F4/80 antibodies. Representative results from 3 individual WT mice in each group are shown in A. Original magnification, ×400. Bar, 50 μm. The numbers of CD4^{+}, or CD8^{+}, CD11c^{+}, or F4/80^{+} cells were counted. Cell density was determined in 10 randomly chosen tumor areas at 400-fold magnification. Mean and SD were calculated and are shown in B and D (n = 5). $^{**}p < 0.01$. (C) RFA-treated tumor tissues were processed using double-color immunofluorescence analysis as described in Materials and Methods. Right panels represent digitally merged images. Representative results from 3 individual animals are shown here. Original magnification, ×400. Bars, 50 μm.

Figure 5. Increased CCL3 expression in RFA-treated tumors.

(A) Real-time RT-PCR was performed on total RNA extracted from RFA-treated tumor of WT mice. The tumors were harvested 6 hours after RFA (left) or 24 hours after RFA (right). Chemokine mRNA level was normalized to GAPDH mRNA levels. Mean and SD were calculated and are shown here (n = 3). $^{*}p < 0.05$ compared with untreated mice. (B) RFA-treated tumors were removed from WT mice on day 1 after RFA plus ECI301 treatment and immunostained with the indicated combinations of antibodies as described in Materials and Methods. The digitally merged images are shown in the right panels. Representative results from 3 individual animals are shown here. Original magnification, ×400. Bars, 50 μm.

Figure 6. ECI301 augmented tumor-specific immune responses after RFA.

(A) Non-RFA-treated tumors were removed from WT mice on day 3 after RFA and immunohistochemical analysis was performed using anti-CD4 or anti-CD8a antibodies. Representative results from 3 individual animals in each group are shown here. Original magnification, ×400. Bar, 50 μm. (B) The number of CD4^{+} or CD8^{+} cells was counted. Cell density was determined in 10 randomly chosen tumor areas at 400-fold magnification. Mean and SD were calculated and are shown here (n = 5). $^{**}p < 0.01$. (C) BALB/c-*nu/nu* mice (left) and BALB/c-WT mice (right) were inoculated with BNL cells and treated as described in the

legend to figure 1. In RFA+ECI301+clodronate liposome (CL) group, the mice were injected with 200μl of CL to deplete monocytes/macrophages as described in Materials and Methods. Non-RFA-treated tumor volumes (mean and SE) were measured twice a week. (D) Spleens from WT, $CCR1^{-/-}$, or $CCR5^{-/-}$ mice were harvested on day 21 after RFA, and mononuclear cells were separated from the spleens for ELISPOT assay as described in Materials and Methods. The numbers of specific spots (mean and SD) were determined by subtracting the number of spots in wells without lysates from the number of spots in wells with tumor lysates (n = 3). *$p < 0.05$; **$p < 0.01$ compared with untreated WT mice.

Figure 1

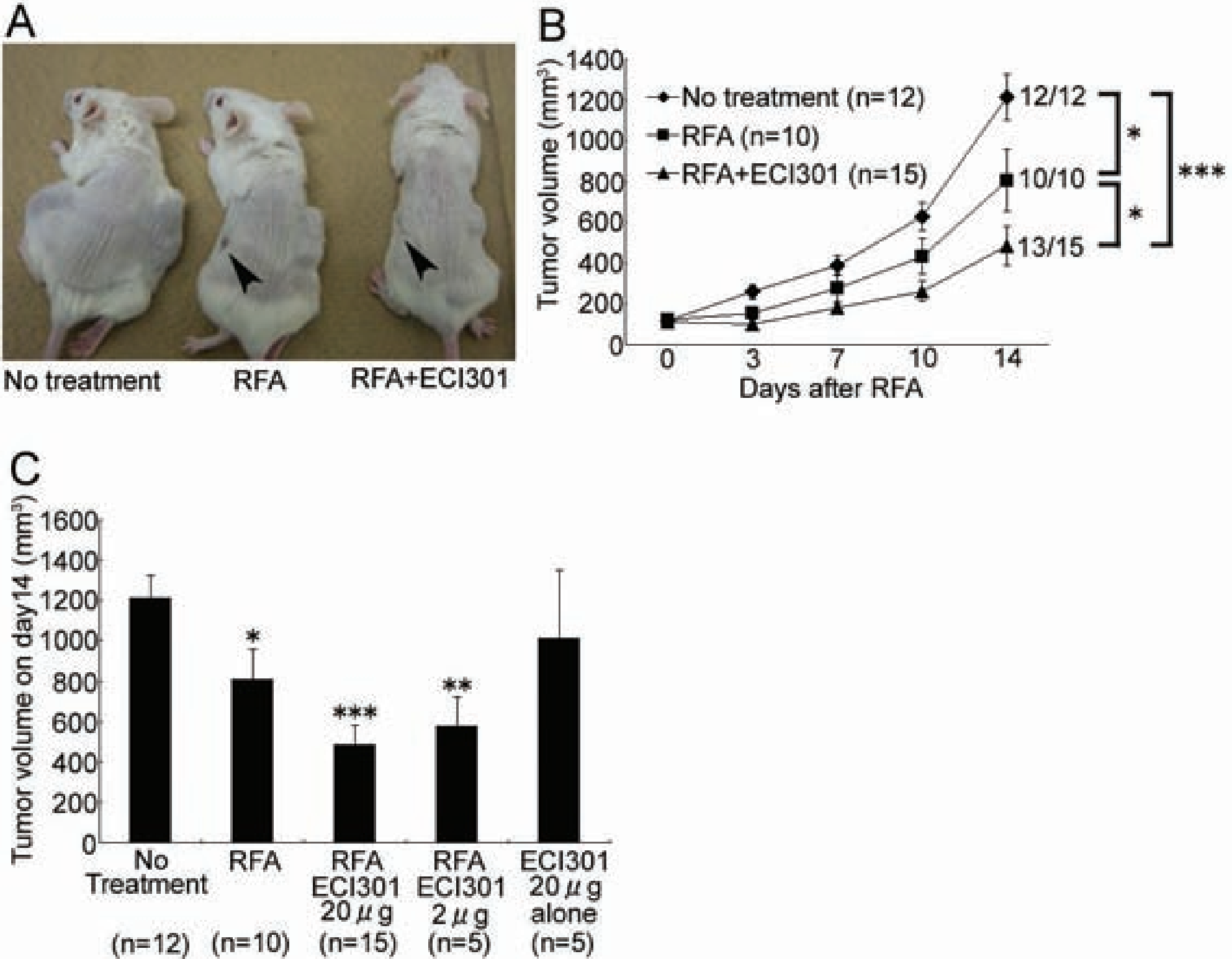
A
No treatment
RFA
RFA+ECI301
B
Tumor volume (mm3)
1400
1200
1000
800
600
400
200
0
No treatment (n=12)
RFA (n=10)
RFA+ECI301 (n=15)
12/12
10/10
13/15
*
*
***
0
3
7
10
14
Days after RFA
C
Tumor volume on day14 (mm3)
1600
1400
1200
1000
800
600
400
200
0
*
***
**
No Treatment
(n=12)
RFA
(n=10)
RFA ECI301 20 μg
(n=15)
RFA ECI301 2 μg
(n=5)
ECI301 20 μg alone
(n=5)

Figure 2

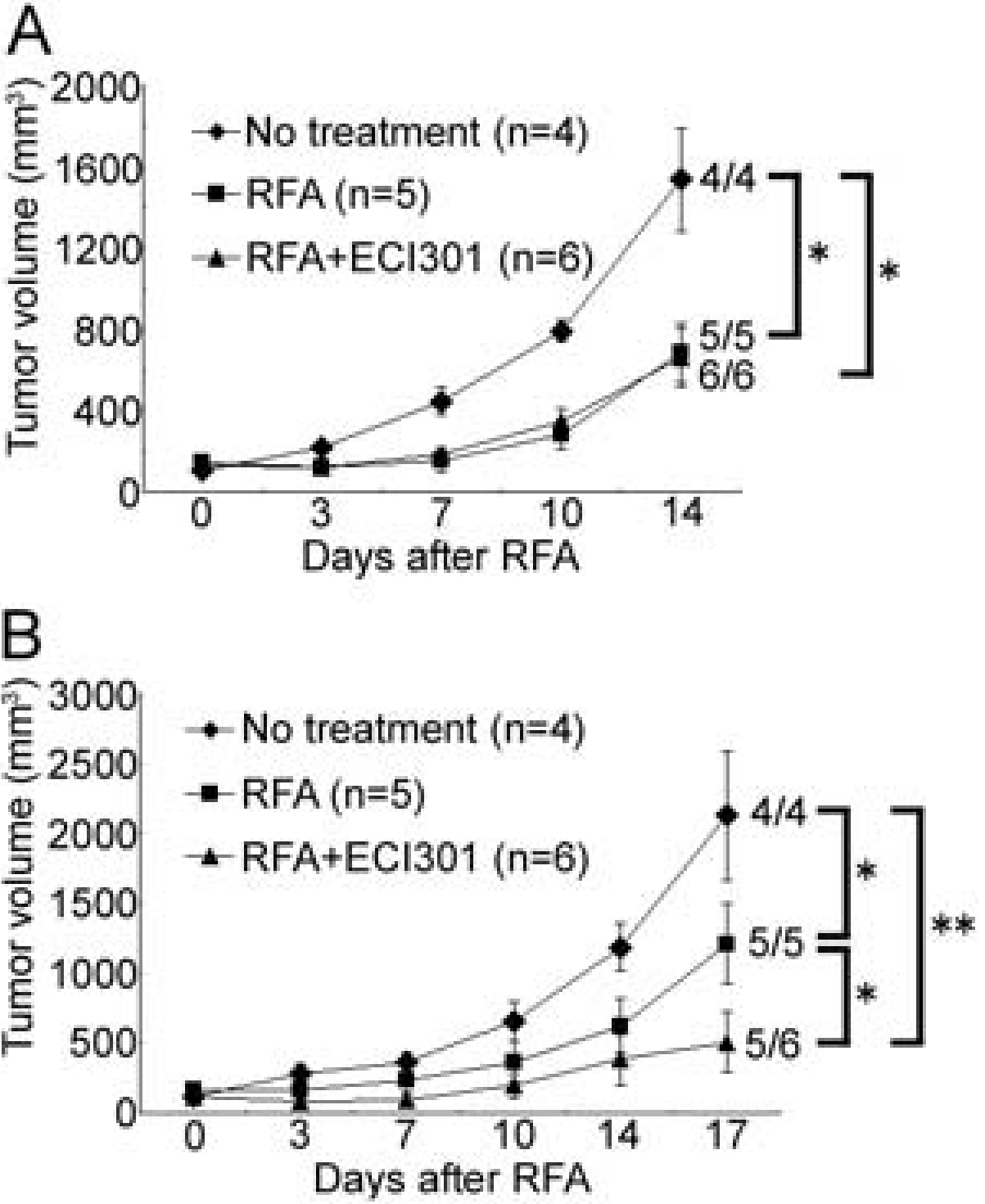
A
Tumor volume (mm³)
2000
1600
1200
800
400
0
No treatment (n=4)
RFA (n=5)
RFA+ECI301 (n=6)
4/4
5/5
6/6
*
*
0
3
7
10
14
Days after RFA
B
Tumor volume (mm³)
3000
2500
2000
1500
1000
500
0
No treatment (n=4)
RFA (n=5)
RFA+ECI301 (n=6)
4/4
5/5
5/6
*
*
**
0
3
7
10
14
17
Days after RFA

Figure 3

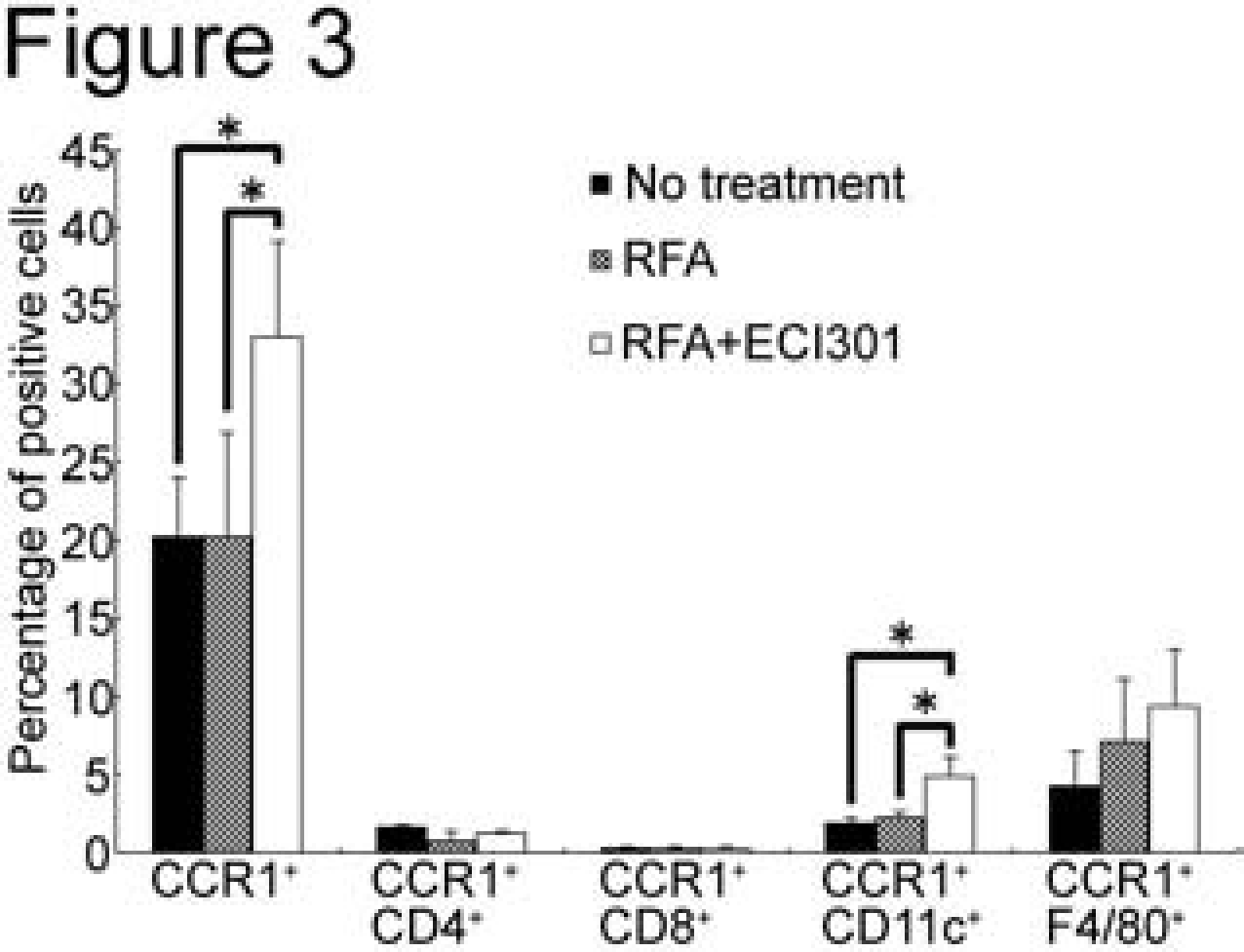
Percentage of positive cells
45
40
35
30
25
20
15
10
5
0
No treatment
RFA
RFA+ECI301
*
*
*
*
CCR1+
CCR1+ CD4+
CCR1+ CD8+
CCR1+ CD11c+
CCR1+ F4/80+

Figure 4

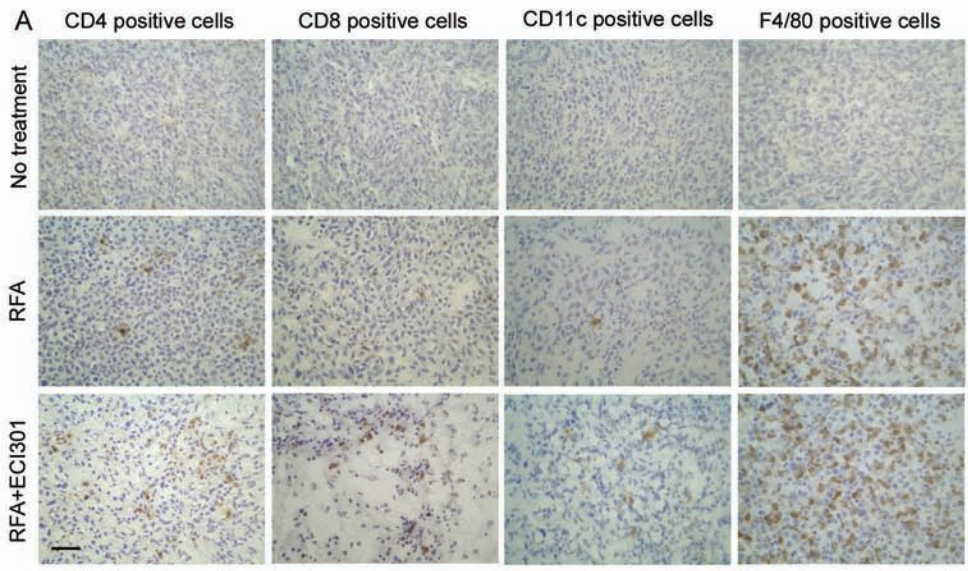
A
CD4 positive cells
CD8 positive cells
CD11c positive cells
F4/80 positive cells
No treatment
RFA
RFA+ECI301

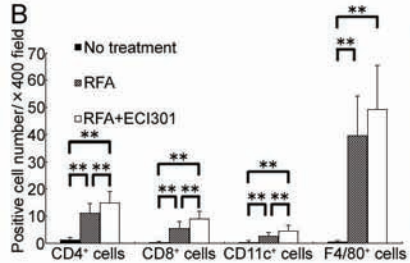
B
No treatment
RFA
RFA+ECI301
Positive cell number/×400 field
CD4+ cells
CD8+ cells
CD11c+ cells
F4/80+ cells

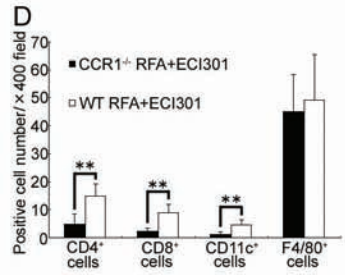
D
CCR1-/- RFA+ECI301
WT RFA+ECI301
Positive cell number/×400 field
CD4+ cells
CD8+ cells
CD11c+ cells
F4/80+ cells

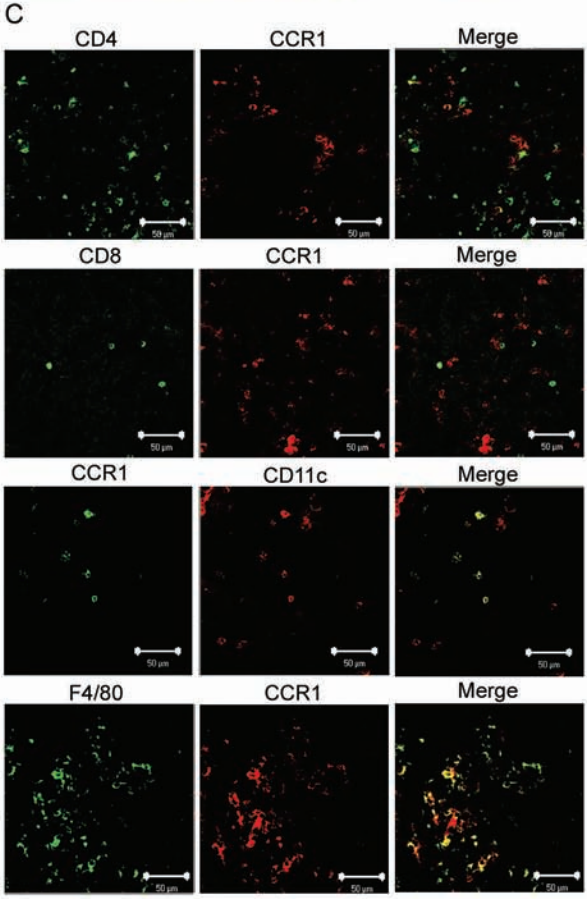
C
CD4
CCR1
Merge
CD8
CCR1
Merge
CCR1
CD11c
Merge
F4/80
CCR1
Merge

Figure 5

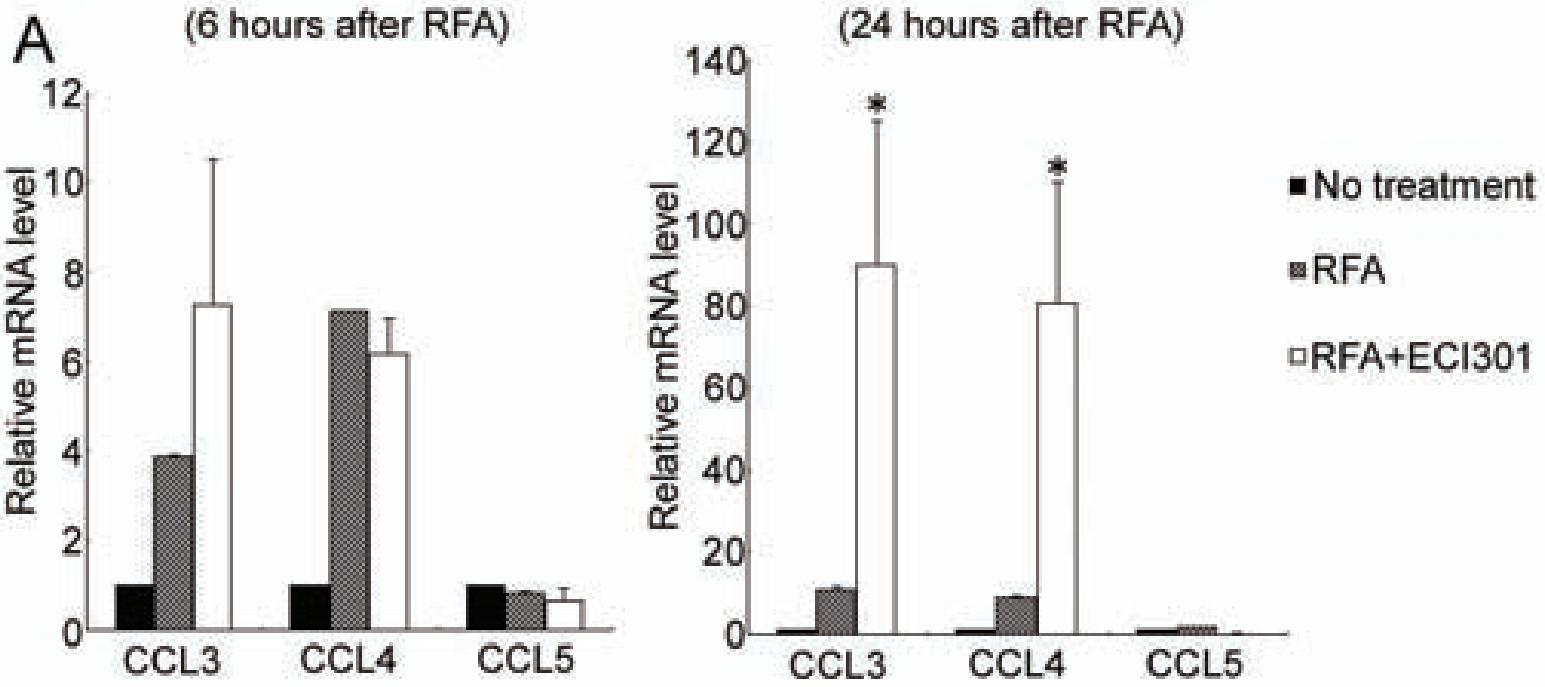
A
(6 hours after RFA)
(24 hours after RFA)
Relative mRNA level
12
10
8
6
4
2
0
140
120
100
80
60
40
20
0
CCL3
CCL4
CCL5
*
*
No treatment
RFA
RFA+ECI301

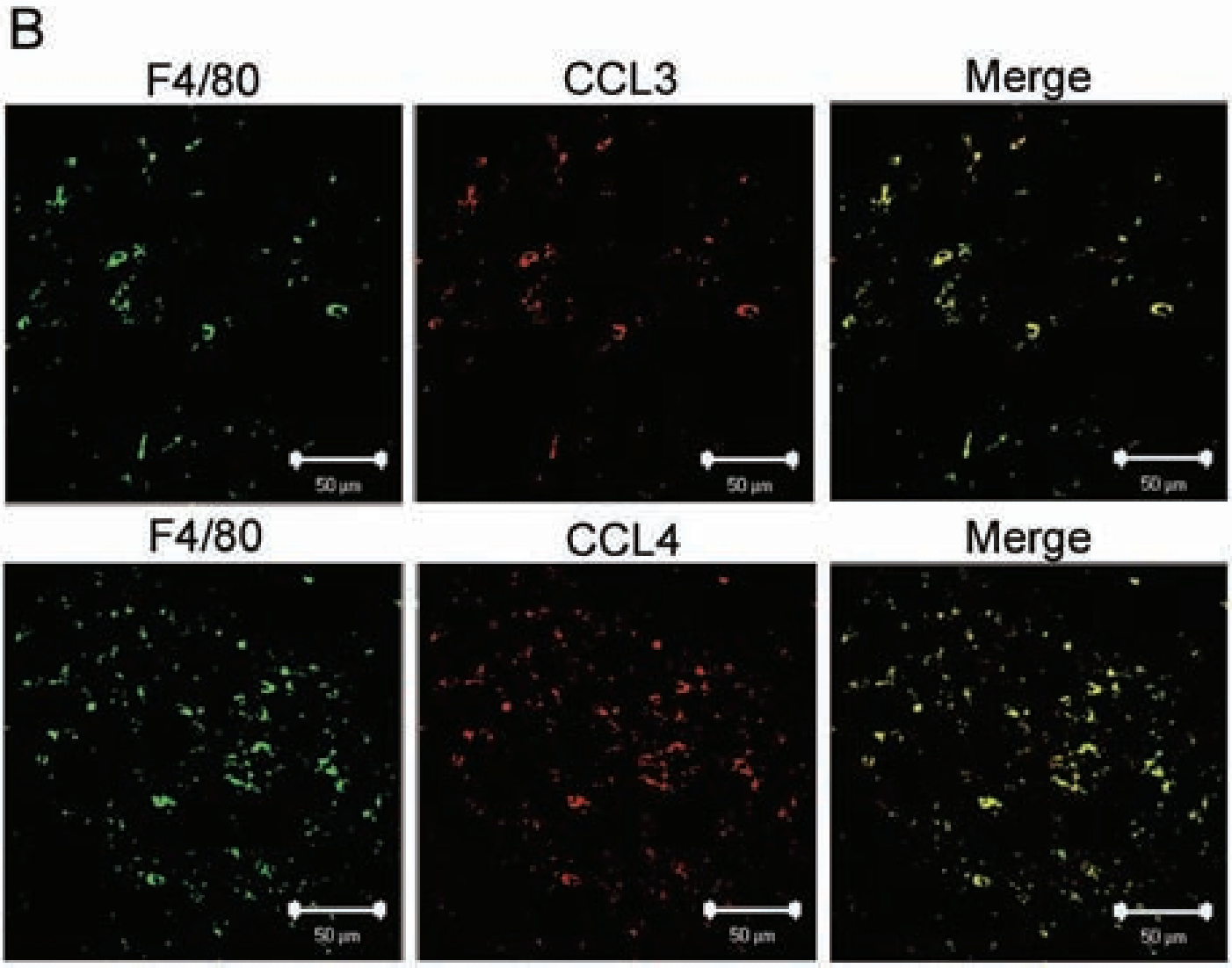
B
F4/80
CCL3
Merge
F4/80
CCL4
Merge
50 μm

Figure 6

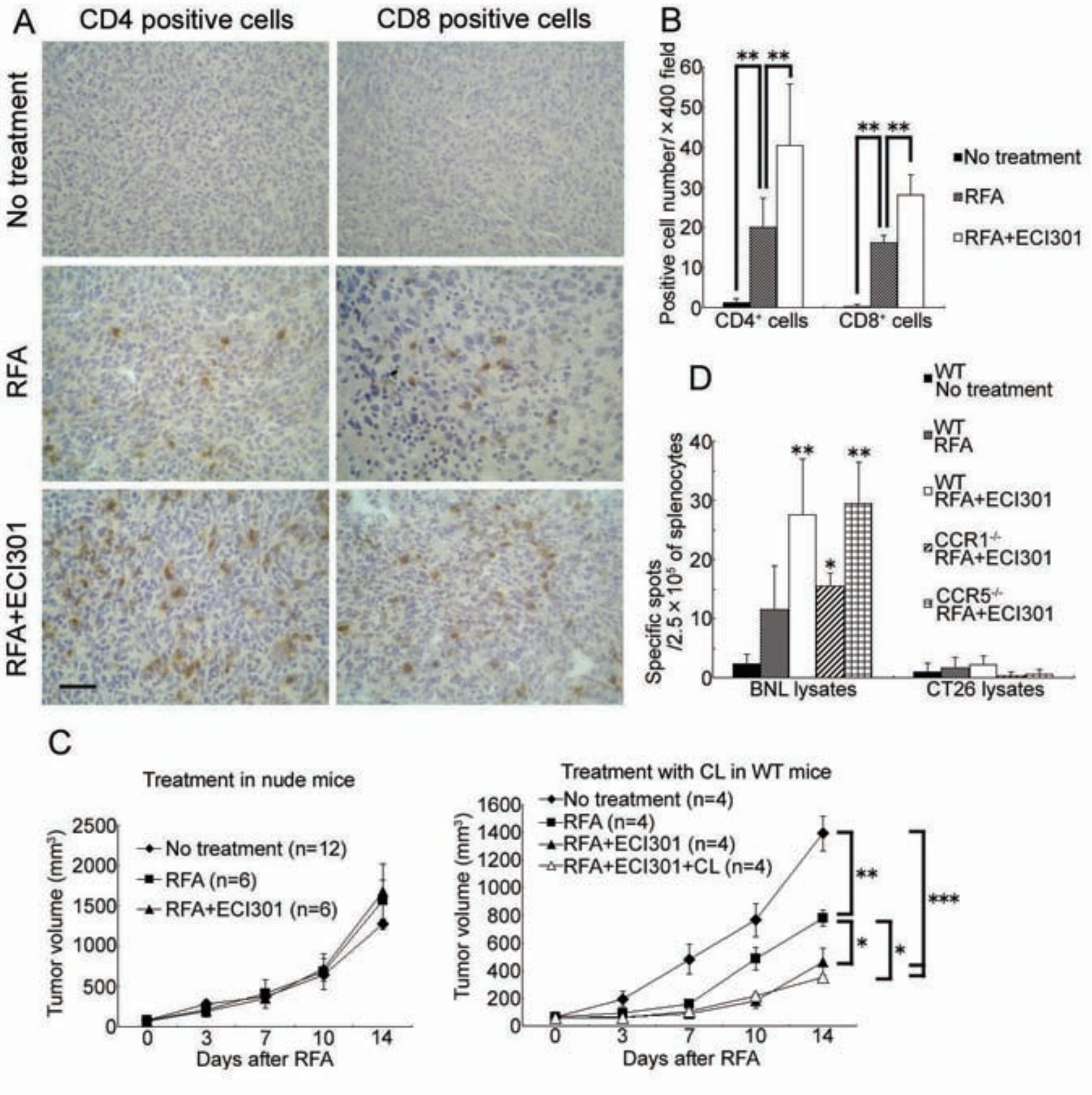
A
CD4 positive cells
CD8 positive cells
No treatment
RFA
RFA+ECI301
B
Positive cell number/ × 400 field
60
50
40
30
20
10
0
** **
** **
CD4⁺ cells
CD8⁺ cells
No treatment
RFA
RFA+ECI301
D
Specific spots /2.5 × 10⁵ of splenocytes
40
30
20
10
0
**
**
*
BNL lysates
CT26 lysates
WT No treatment
WT RFA
WT RFA+ECI301
CCR1⁻/⁻ RFA+ECI301
CCR5⁻/⁻ RFA+ECI301
C
Treatment in nude mice
Tumor volume (mm³)
2500
2000
1500
1000
500
0
No treatment (n=12)
RFA (n=6)
RFA+ECI301 (n=6)
0
3
7
10
14
Days after RFA
Treatment with CL in WT mice
Tumor volume (mm³)
1600
1400
1200
1000
800
600
400
200
0
No treatment (n=4)
RFA (n=4)
RFA+ECI301 (n=4)
RFA+ECI301+CL (n=4)
**
*
*
***
0
3
7
10
14
Days after RFA